

GigaScience

A highly predictive signature of cognition and brain atrophy for progression to Alzheimer's dementia --Manuscript Draft--

Manuscript Number:	GIGA-D-18-00349	
Full Title:	A highly predictive signature of cognition and brain atrophy for progression to Alzheimer's dementia	
Article Type:	Research	
Funding Information:	Canadian Network for Research and Innovation in Machining Technology, Natural Sciences and Engineering Research Council of Canada (CA) (RN000028)	Dr Pierre Bellec
	Courtois Foundation (n/a)	Dr Pierre Bellec
	Lemaire Foundation (n/a)	Dr Pierre Bellec
Abstract:	<p>Patients with mild cognitive impairment (MCI) are at risk of progressing to Alzheimer's dementia, yet only a fraction of them do. We explore here whether a very high-risk MCI subgroup can be identified using cognitive assessments and structural neuroimaging. A multimodal signature of Alzheimer's dementia was first extracted using machine learning tools in the ADNI1 sample, and was comprised of cognitive deficits across multiple domains as well as atrophy in temporal, parietal and occipital regions. We then validated the predictive value of this signature on two MCI cohorts. In ADNI1 (N=235), the presence of the signature predicted progression to dementia over three years with 80.4% positive predictive value, adjusted for a "typical" MCI baseline rate of 33% (95.6% specificity, 55.1% sensitivity). These results were replicated in ADNI2 (N=235), with 87.8% adjusted positive predictive value (96.7% specificity, 47.3% sensitivity). Our results demonstrate that, even for widely used markers, marked improvement in positive predictive value over the literature can be achieved by focusing on a subgroup of individuals with similar brain characteristics. The signature can be readily applied for the enrichment of clinical trials.</p>	
Corresponding Author:	Angela Tam, PhD Centre de recherche de l'institut universitaire de gériatrie de Montréal Montreal, Quebec CANADA	
Corresponding Author Secondary Information:		
Corresponding Author's Institution:	Centre de recherche de l'institut universitaire de gériatrie de Montréal	
Corresponding Author's Secondary Institution:		
First Author:	Angela Tam, PhD	
First Author Secondary Information:		
Order of Authors:	Angela Tam, PhD	
	Christian Dansereau, PhD	
	Yasser Iturria-Medina, PhD	
	Sebastian Urchs, MSc	
	Pierre Orban, PhD	
	Hanad Sharmarke, BSc	
	John Breitner, MD	
	Pierre Bellec, PhD	

Order of Authors Secondary Information:	
Additional Information:	
Question	Response
Are you submitting this manuscript to a special series or article collection?	No
<p>Experimental design and statistics</p> <p>Full details of the experimental design and statistical methods used should be given in the Methods section, as detailed in our Minimum Standards Reporting Checklist. Information essential to interpreting the data presented should be made available in the figure legends.</p> <p>Have you included all the information requested in your manuscript?</p>	Yes
<p>Resources</p> <p>A description of all resources used, including antibodies, cell lines, animals and software tools, with enough information to allow them to be uniquely identified, should be included in the Methods section. Authors are strongly encouraged to cite Research Resource Identifiers (RRIDs) for antibodies, model organisms and tools, where possible.</p> <p>Have you included the information requested as detailed in our Minimum Standards Reporting Checklist?</p>	Yes
<p>Availability of data and materials</p> <p>All datasets and code on which the conclusions of the paper rely must be either included in your submission or deposited in publicly available repositories (where available and ethically appropriate), referencing such data using a unique identifier in the references and in the “Availability of Data and Materials” section of your manuscript.</p>	Yes

Have you have met the above requirement as detailed in our [Minimum Standards Reporting Checklist](#)?

Click here to view linked References

A highly predictive signature of cognition and brain atrophy for progression to Alzheimer's dementia

Short running title: Signature of future Alzheimer's dementia

Angela Tam^{1,2,3,†}, Christian Dansereau^{1,4}, Yasser Itturia-Medina³, Sebastian Urchs³, Pierre Orban^{1,5,6}, Hanad Sharmarke¹, John Breitner^{2,3}, Pierre Bellec^{1,4,†}, for the Alzheimer's Disease Neuroimaging Initiative*

1. Centre de Recherche de l'Institut Universitaire de Gériatrie de Montréal, Montréal, CA
2. Douglas Hospital Research Centre, McGill University, Montréal, CA
3. McGill University, Montréal, CA
4. Département d'Informatique et de recherche opérationnelle, Université de Montréal, Montréal, CA
5. Centre de Recherche de l'Institut Universitaire en Santé Mentale de Montréal, Montréal, CA
6. Département de Psychiatrie, Université de Montréal, Montréal, CA

*Data used in preparation of this article were obtained from the Alzheimer's Disease Neuroimaging Initiative (ADNI) database (adni.loni.usc.edu). As such, the investigators within the ADNI contributed to the design and implementation of ADNI and/or provided data but did not participate in analysis or writing of this report. A complete listing of ADNI investigators can be found at: http://adni.loni.usc.edu/wp-content/uploads/how_to_apply/ADNI_Acknowledgement_List.pdf

†Corresponding authors:

angela.tam@mail.mcgill.ca

pierre.bellec@criugm.qc.ca

4545 Queen Mary Rd

Montreal QC

Canada H3W 1W6

Abstract

1
2
3 30 Patients with mild cognitive impairment (MCI) are at risk of progressing to Alzheimer's
4 dementia, yet only a fraction of them do. We explore here whether a very high-risk MCI
5 subgroup can be identified using cognitive assessments and structural neuroimaging. A
6 32 multimodal signature of Alzheimer's dementia was first extracted using machine learning
7 tools in the ADNI1 sample, and was comprised of cognitive deficits across multiple domains
8 as well as atrophy in temporal, parietal and occipital regions. We then validated the predictive
9 value of this signature on two MCI cohorts. In ADNI1 (N=235), the presence of the signature
10 predicted progression to dementia over three years with 80.4% positive predictive value,
11 34 adjusted for a "typical" MCI baseline rate of 33% (95.6% specificity, 55.1% sensitivity).
12 These results were replicated in ADNI2 (N=235), with 87.8% adjusted positive predictive
13 value (96.7% specificity, 47.3% sensitivity). Our results demonstrate that, even for widely
14 used markers, marked improvement in positive predictive value over the literature can be
15 36 achieved by focusing on a subgroup of individuals with similar brain characteristics. The
16 signature can be readily applied for the enrichment of clinical trials.
17
18 38
19
20
21
22 40
23
24
25
26 42
27
28
29
30

44 Keywords

31
32 Alzheimer's disease, mild cognitive impairment, machine learning, neuroimaging, cognition
33
34
35
36
37
38
39
40
41
42
43
44
45
46
47
48
49
50
51
52
53
54
55
56
57
58
59
60
61
62
63
64
65

46 Introduction

1 Alzheimer's disease (AD), a leading cause of dementia, is marked by the abnormal
2
3 accumulation of amyloid β ($A\beta$) and hyperphosphorylated tau proteins in the brain, which
4 48
5 leads to widespread neurodegeneration. AD has a long prodromal phase, and it has been
6
7 difficult to predict which individuals will decline and experience AD dementia. While mild
8 50
9 cognitive impairment (MCI) is often considered a prodromal stage of AD, only a fraction (up
10
11 to 36%) of MCI patients will develop dementia within two years [1]. Identifying MCI
12 52
13 patients who will progress to AD dementia with enough specificity has been a challenge for
14
15 clinical trials, where the inclusion criteria for MCI subjects have had low to moderate positive
16 54
17 predictive value (PPV) [2]. This lack of prognostic power may be due to individual
18
19 variability. Different clinical phenotypes have been described where patients will exhibit
20 56
21 distinct cognitive deficits [3]. Previous work has also characterized neuropathological
22
23 subtypes based on the distribution of neurofibrillary tangles [4], which correspond well to
24 58
25 distinct patterns of brain atrophy [5]. Different subtypes of brain atrophy have also been
26
27 associated with different rates of progression to dementia [6]. The implications for prognosis
28 60
29 are profound: only a subgroup of patients will have clinical trajectories that can be reliably
30
31 predicted. We therefore propose to identify a subset of individuals with a homogenous
32 62
33 signature of brain atrophy and cognitive deficits who will progress to AD dementia with high
34
35 precision.
36 64

36
37 There is a large field focused on using machine learning to automatically detect MCI
38 66
39 patients who will progress to AD dementia based on imaging and cognitive features. For
40
41 models combining structural MRI and cognition, in terms of accuracy, the best has been
42 68
43 reported at 79% (76% specificity, 83% sensitivity) [7]. The state-of-the-art, which used $A\beta$
44
45 positron emission tomography scans, has so far achieved 82% accuracy (87% specificity,
46 70
47 71% sensitivity) [8]. Note that accuracy is defined as the proportion of subjects that were
48
49 correctly identified, either as positives or negatives. PPV, on the other hand, is defined as the
50 72
51 proportion of true positives out of all subjects that were classified as positive. A model can
52
53 have high accuracy yet moderate PPV if the proportion of true positives is low relative to true
54 74
55 negatives. In the case of predicting incipient AD, relatively few MCI subjects progress to
56
57 dementia. Despite promising accuracy, the PPVs of models predicting AD progression remain
58 76
59 moderate, ranging from 50 to 75% across the literature [9]. This implies that up to half of
60
61 subjects who were identified as progressors by published algorithms did not actually progress
62
63
64
65

78 to dementia. It seems that by focussing our efforts on improving accuracy, we have a reached
1 a plateau in generating models with good precision. We therefore aimed to create a predictive
2
3
4 80 model that was optimized for high PPV.

5
6 In this work, we developed a multimodal signature that is highly predictive of
7
8 82 progression to AD dementia in a subgroup of MCI patients, based on cognition and subtypes
9
10 of grey matter atrophy. We also aimed to evaluate the complementarity of features derived
11
12 84 from cognition and atrophy patterns. Although this has been extensively studied for prognosis
13
14 of dementia in a general MCI population, the complementarity of these measures is not
15
16 86 documented in the specific context of a high risk signature. We applied a cluster analysis on
17
18 structural magnetic resonance images to identify subtypes of brain atrophy in a sample
19
20 88 containing both patients with AD dementia and cognitively normal (CN) individuals. We then
21
22 used a two-step machine learning algorithm [9] to train a model to identify three signatures
23
24 90 that were highly predictive of AD dementia: 1) an anatomical signature, 2) a cognitive
25
26 signature, 3) a multimodal anatomical and cognitive signature. After identifying MCI patients
27
28 92 carrying these signatures, we examined cognitive decline, $A\beta$ and tau burden, and
29
30 progression to dementia in these individuals to explore whether a highly predictive signature
31
32 94 represented a prodromal stage of AD. We analysed whether these three signatures identified
33
34 separate subgroups of subjects and how they performed against each other in terms of PPV,
35
36 96 specificity, and sensitivity at identifying progressors.

38 **Materials and methods**

40 98 **Data**

41
42 Data used in the preparation of this article were obtained from the Alzheimer's
43
44 100 Disease Neuroimaging Initiative (ADNI) database (adni.loni.usc.edu). The ADNI was
45
46 launched in 2003 as a public-private partnership, led by Principal Investigator Michael W.
47
48 102 Weiner, MD. The primary goal of ADNI has been to test whether serial magnetic resonance
49
50 imaging (MRI), positron emission tomography (PET), other biological markers, and clinical
51
52 104 and neuropsychological assessment can be combined to measure the progression of mild
53
54 cognitive impairment (MCI) and early Alzheimer's disease (AD). For up-to-date information,
55
56 106 see www.adni-info.org.

1 We took baseline T1-weighted MRI scans from the ADNI1 (228 CN, 397 MCI, 192
2 108 AD) and ADNI2 (218 CN, 354 MCI, 103 AD) studies. For a detailed description of MRI
3 acquisition details, see <http://adni.loni.usc.edu/methods/documents/mri-protocols/>. All
4 subjects gave informed consent to participate in these studies, which were approved by the
5 110 research ethics committees of the institutions involved in data acquisition. Consent was
6 obtained for data sharing and secondary analysis, the latter being approved by the ethics
7 committee at the CRIUGM. For the MCI groups, each individual must have had at least 36
8 months of follow-up for inclusion in our analysis. We also further stratified the MCI groups
9 112 into stable (sMCI), who never received any change in their diagnosis, and progressors
10 (pMCI), who received a diagnosis of AD dementia within 36 months of follow-up. pMCI
11 who progressed to AD dementia after 36 months were excluded. After applying these
12 inclusion/exclusion criteria, we were left with 280 and 268 eligible MCI subjects in ADNI1
13 114 and ADNI2 respectively.

26 120 **Structural features from voxel-based morphometry**

29 Images were processed with the NeuroImaging Analysis Kit (NIAK) version 0.18.1
30 122 (<https://hub.docker.com/r/simexp/niak-boss/>), the MINC toolkit (<http://bic-mni.github.io/>)
31 version 0.3.18, and SPM12 (<http://www.fil.ion.ucl.ac.uk/spm/software/spm12/>) under
32 CentOS with Octave (<http://gnu.octave.org>) version 4.0.2. Preprocessing of MRI data was
33 124 executed in parallel on the Cedar supercomputer (<https://docs.computecanada.ca/wiki/Cedar>),
34 using the Pipeline System for Octave and Matlab (PSOM) [10]. Each T1 image was linearly
35 126 co-registered to the Montreal Neurological Institute (MNI) ICBM152 stereotaxic symmetric
36 template [11], using the CIVET pipeline [12], and then re-oriented to the AC-PC line. Each
37 image was segmented into grey matter, white matter, and CSF probabilistic maps. The
38 128 DARTEL toolbox [13] was used to normalize the grey matter segmentations to a predefined
39 grey matter template in MNI152 space. Each map was modulated to preserve the total amount
40 of signal and smoothed with with a 8 mm isotropic Gaussian blurring kernel. After quality
41 control of the normalized grey matter segmentations, we were left with 621 subjects in
42 130 ADNI1 (out of 700, 88.7% success rate) and 515 subjects in ADNI2 (out of 589, 87.4%
43 success rate).

57 136 We extracted subtypes to characterize variability of grey matter distribution with the
58 CN and AD samples from ADNI1. In order to reduce the impact of factors of no interest that

138 may have influenced the clustering procedure, we regressed out age, sex, mean grey matter
1 volume (GMV), and total intracranial volume (TIV), using a mass univariate linear regression
2 model at each voxel. We then derived a spatial Pearson's correlation coefficient between all
3
4 140 pairs of individual maps after confound regression. This defined a subject x subject (377 x
5
6
7 142 377) similarity matrix which was entered into a Ward hierarchical clustering procedure
8
9 (Figure 1a). Based on visual inspection of the similarity matrix, we identified 7 subgroups
10 (Figure 1b). Each subtype was defined as the average map of each subgroup. For each
11 144 subject, we computed spatial correlations between their map and each subtype, which we call
12
13 weights (Figure 1a). The weights formed a n subject x n subtypes matrix, which was included
14
15 146 in the feature space for all predictive models including VBM throughout this work. As in our
16
17 previous works [9,14], we chose to use weights, which can be interpreted as continuous
18
19 148 measures for subtype affinity, over discrete subtype membership because the latter is less
20
21 informative as most individuals express similarity to multiple subtypes [15]. Note that
22
23 150 although we chose to present our findings with 7 subtypes, we examined how the number of
24
25 subtypes may impact our subsequent predictions. There was no significant difference in
26
27 152 model performance when we changed the number of subtypes (see Table S1 in supplementary
28
29 material).
30 154
31
32
33

34 **Cognitive features**

35
36 156 We took baseline neuropsychological scores for each subject from several cognitive
37 domains: memory from the composite score ADNI-MEM [16], executive function from the
38 composite score ADNI-EF [17], language from the Boston Naming Test (BNT), visuospatial
39
40 158 from the clock drawing test, and global cognition from the Alzheimer's Disease Assessment
41 Scale-Cognitive (ADAS13). We chose measures that span multiple cognitive domains as it
42
43 has been suggested that the use of a combination of neuropsychological measures is likely the
44 160 best approach to predicting incipient dementia [18]. These scores were included as features
45
46 for the predictive models involving cognition. Thirteen subjects across both ADNI1 and
47
48 162 ADNI2 (8 AD, 5 MCI) had to be excluded due to missing values in their cognitive
49
50 assessments. See Table 1 for demographic information of subjects who were included in
51
52 164 analyses.
53
54
55
56 166
57
58
59
60
61
62
63
64
65

Prediction of easy AD dementia cases in ADNI1

We trained a linear support vector machine (SVM) model with a linear kernel, as implemented by Scikit-learn [19] version 0.18 to classify AD vs CN from ADNI1 to get a baseline prediction accuracy. A tenfold cross-validation loop was used to estimate the performance of the trained model. Classes were balanced inversely proportional to class frequencies in the input data for the training. A nested cross-validation loop (stratified shuffle split with 50 splits and 20% test size) was used for the grid search of the hyperparameter C (grid was 10^{-2} to 10^1 with 15 equal steps). We randomly selected subsamples of the dataset (retaining 50% of participants in each subsample) to replicate the SVM training 500 times. For each 50% subsample, a separate SVM model was trained to predict AD or CN in ADNI1. Predictions were made on the remaining 50% of the sample that was not used for training. For each subject, we calculated a hit probability defined as the frequency of correct classification across all SVM replications in which the test set contained that subject. Easy AD cases were defined as individuals with 100% hit probabilities with the AD label. Next, we trained a logistic regression classifier [20], with L1 regularization on the coefficients, to predict the easy AD cases. A stratified shuffle split (500 splits, 50% test size) was used to estimate the performance of the model for the grid search of the hyperparameter C (grid was 10^{-2} to 10^1 with 15 equal steps). See [9] for more information about this two-step prediction. We used the whole CN and AD sample from ADNI1 to obtain three highly predictive signatures (HPS), one using VBM subtypes (VBM only), one using cognitive features (COG only), and one using the combination of VBM and cognitive features (VCOG). In all three signatures, age, sex, mean GMV, and TIV were also included as features.

Prediction of progression to AD dementia from the MCI stage in ADNI1

The logistic regression trained on AD vs CN was used to identify MCI patients who have a HPS of AD dementia in ADNI1. We re-trained our models on AD vs CN after optimizing our hyperparameters (resampling size and resampling ratio) in order to maximize specificity and PPV while keeping a minimum of 30% sensitivity for our classification of sMCI (n=89) vs pMCI (n=155) in ADNI1. This was done for all three signatures. In brief, we

1
2 196 used the AD and CN sample from ADNI1 as a training set, the MCI subjects from ADNI1 as
3
4
5
6 a validation set, and ADNI2 served as our test set.

7 8 198 **Statistical test of differences in model performance**

9
10 We used Monte-Carlo simulations to generate confidence intervals on the
11 200 performance (i.e. PPV, specificity and sensitivity) of both base SVM and HPS models for
12 their predictions of AD vs CN and pMCI vs sMCI. Taking the observed sensitivity and
13 specificity, and using similar sample sizes to our experiment, we replicated the number of
14 true and false positive detection 100000 times using independent Bernoulli variables, and
15 202 derived replications of PPV, specificity and sensitivity. By comparing these replications to the
16 sensitivity, specificity and PPV observed in both models, we estimated a p-value for
17 differences in model performance [21]. A p-value smaller than 0.05 was interpreted as
18 evidence of a significant difference in performance, and 0.001 as strong evidence. We also
19 204 used this approach to compare the performance of the combined features (VCOG) to the
20 models containing VBM features or cognitive features only. Note that, based on our
21 hypotheses regarding the behaviour of the HPS model, the tests were one-sided for increased
22 specificity and PPV, and one-sided for decreased sensitivity.
23 206
24
25
26
27 208
28
29
30
31 210
32
33

34 35 **Statistical tests of association of progression, AD biomarkers, and risk factors in** 36 212 **HPS+ MCI subjects**

37
38 Based on the classifications resulting from the base SVM and HPS models, we
39 separated the MCI subjects into three different groups: 1) HPS+, subjects who were selected
40 214 by the HPS model as hits, 2) Non-HPS+, subjects who were selected by the base SVM model
41 as hits but were not selected by the HPS model, and 3) Negative, subjects who were not
42 216 selected as hits by either algorithm.
43
44
45
46
47

48 218 We tested statistically if the HPS+ subgroup was enriched for progression to
49 dementia, APOE4 carriers, females, and subjects who were positive for A β and tau pathology.
50 Positivity of AD pathology was determined by CSF measurements of A β 1-42 peptide and
51 220 total tau with cut-off values of less than 192 pg/mL and greater than 93 pg/mL respectively
52 [22]. We implemented Monte-Carlo simulations, where we selected 100000 random
53 subgroups out of the original MCI sample. By comparing the proportion of progressors,
54
55
56 222
57
58
59
60
61
62
63
64
65

224 APOE4 carriers, females, $A\beta$ -positive, and tau-positive subjects in these null replications to
1 the actual observed values in the HPS subgroup, we estimated a p-value [21] (one sided for
2 increase). A p-value smaller than 0.05 was interpreted as evidence of a significant
3
4 226 enrichment, and 0.001 as strong evidence.
5
6

7 228 One-way ANOVAs were used to evaluate differences between the HPS groupings
8 with respect to age. Post-hoc Tukey's HSD tests were done to assess pairwise differences
9
10 among the three classes (HPS+, Non-HPS+, Negative). These tests were implemented in
11 230 Python with the SciPy library [23] version 0.19.1 and StatsModels library [24] version 0.8.0.
12
13

14 232 To explore the impact of HPS grouping on cognitive trajectories, linear mixed effects
15 models were performed to evaluate the main effects of and interactions between the HPS
16
17 groups and time on ADAS13 scores up to 36 months of follow-up. The models were first fit
18 234 with a random effect of participant and then were fit with random slopes (time | participant) if
19 ANOVAs comparing the likelihood ratio suggested a significant improvement in model fit.
20
21 All tests were performed separately on the ADNI1 and ADNI2 datasets. These tests were
22 236 implemented in R version 3.3.2 with the library nlme version 3.1.128 [25].
23
24
25
26
27
28
29
30

31 **Public code and data availability**

32 240 The code used in this experiment is available on a GitHub repository
33 (https://github.com/SIMEXP/vcog_hps_ad) and zenodo
34
35 (<https://doi.org/10.5281/zenodo.1444081>).
36 242

37
38 We shared a notebook replicating all the machine learning experiments, starting after
39
40 244 the generation of VBM subtypes. However, in order to protect the privacy of the study
41 participants, we could not share individual subtype weights alongside other behavioural data
42 and diagnostic information. We thus created parametric (Gaussian) bootstrap simulations,
43 246 based on group statistics alone, that will allow interested readers to replicate results similar to
44 those presented in this manuscript, using the exact same code and computational environment
45
46 that were used on real data, but with purely synthetic data instead. The notebook can be
47 248 executed online via the binder platform (<http://mybinder.org>), and runs into a docker
49 container
50
51 ([https://mybinder.org/v2/gh/HanadS/vcog_hps_ad/master?filepath=%2Fvcog_hpc_prediction
52 250 simulated_data.ipynb](https://mybinder.org/v2/gh/HanadS/vcog_hps_ad/master?filepath=%2Fvcog_hpc_prediction_simulated_data.ipynb)), built from a configuration file that is available on GitHub
53
54
55
56
57
58
59
60
61
62
63
64
65

254 (https://github.com/SIMEXP/vcog_hps_ad/blob/master/Dockerfile). The container itself is
1 available on Docker Hub (https://hub.docker.com/r/simexp/vcog_hps_ad/). The simulated
2
3
4 256 data was archived on figshare
5
6 ([https://figshare.com/articles/Simulated_cognitive_and_structural_MRI_data_from_ADNI/71](https://figshare.com/articles/Simulated_cognitive_and_structural_MRI_data_from_ADNI/7132757)
7 258 [32757](https://figshare.com/articles/Simulated_cognitive_and_structural_MRI_data_from_ADNI/7132757)).

9 The simulation included the following 16 variables: age, sex, mean grey matter
10
11 260 volume, total intracranial volume, 5 cognitive assessment scores and 7 VBM subtype weights
12
13 from both ADNI1 and ADNI2. Subjects that had missing values for these variables were
14
15 262 discarded from the simulation, leaving N=1115 subjects. We stratified the population into 12
16
17 subgroups: the four clinical labels (AD, pMCI, sMCI, CN), each further subdivided by the
18
19 264 three prediction subclasses identified in this paper (Negative, Non-HPS+, HPS+). For each
20
21 subgroup, we estimated the average and covariance matrices between the 16 variables of
22
23 266 interest. We then generated a number of multivariate normal data points that matched the
24
25 number of subjects found in each subgroup, using the empirical mean and covariance matrix
26
27 268 of each subgroup. Finally, the range of the simulated data was clipped to the range of the
28
29 original real data, and the simulated sex data points were binarized by nearest neighbour.

30 270 The statistics from the predictive model in the original implementation are similar to
31
32 that of the simulated data. The model predicted the progression of dementia from MCI in
33
34 272 ADNI1 with a PPV of 93.1% (specificity of 93.2%) on real data. This coincides with a 93.3%
35
36 PPV (specificity of 94.3%) that we get when using the simulated data. Similarly, with the
37
38 274 ADNI2 dataset the model achieved a 81.3% PPV (specificity of 96.7%) from the real data
39
40 and a 75.7% PPV (specificity of 95.0%) from the simulated data.
41
42
43

44 276 **Results**

45 46 **Prediction of AD dementia vs cognitively normal individuals** 47

48 278 The SVM model trained using the VCOG features achieved 94.5% PPV (95.6%
49
50 specificity, 93.9% sensitivity) when classifying AD vs CN in ADNI1. Such high performance
51
52 280 was expected given the marked cognitive deficits associated with clinical dementia. COG
53
54 features only actually reached excellent performance as well (97.6% PPV, 98.0% specificity,
55
56 282 96.4% sensitivity), while using VBM features only yielded markedly lower performances
57
58 (86.4% PPV, 89.3% specificity, 79.6% sensitivity) (see Figure 2a). Note that the performance
59
60
61
62
63
64
65

284 metrics in ADNI1 were estimated through cross-validation, and represent an average
1 performance for several models trained on different subsets of ADNI1. We then trained a
2
3
4 286 model on all of ADNI1, and estimated its performance on an independent dataset, ADNI2.
5
6 Using VCOG predictors, the ADNI1 model reached 92.0% PPV (96.3% specificity, 92.0%
7
8 288 sensitivity), when applied on ADNI2 AD vs CN data. Again the performance was comparable
9
10 with COG predictors only (92.2% PPV, 96.3% specificity, 94.3% sensitivity), and lower
11
12 290 performance with VBM features only (57.3% PPV, 79.8% specificity, 56.7% sensitivity) (see
13
14 Figure 2a). Note that PPV is dependent on the proportion of patients and controls for a given
15
16 292 sensitivity and specificity. Since the ADNI2 sample had a substantially smaller proportion of
17
18 AD subjects compared to ADNI1, the resulting PPV was reduced. When we adjusted the
19
20 294 baseline rate of AD subjects in ADNI2 to the same rate in ADNI1, the PPVs were 95.2%,
21
22 95.3%, and 70.2% for the VCOG, COG, and VBM models respectively.
23
24

25 296 **Identification of easy AD cases for prediction**

26
27 The VCOG HPS model achieved 99.2% PPV (99.5% specificity, 77.6% sensitivity) in
28
29 298 classifying easy AD subjects in ADNI1. These performance scores were estimated by
30
31 cross-validation of the entire two-stage process (training of SVM, estimation of hit
32
33 300 probability, identification of HPS). However, the hyperparameters of the two-stage model
34
35 were optimized on classifying pMCI vs sMCI in ADNI1, as described below. We next trained
36
37 302 a single model on all of ADNI1, which we applied on an independent sample (ADNI2). The
38
39 ADNI1 AD VCOG HPS model reached 98.6% PPV (99.5% specificity, 79.5% sensitivity) on
40
41 304 ADNI2. As was previously observed with the conventional SVM analysis, the VCOG HPS
42
43 model had similar performance to the COG HPS model (ADNI1: 100% PPV, 100%
44
45 306 specificity, 87.3% sensitivity; ADNI2: 98.7% PPV, 99.5% specificity, 88.6% sensitivity), and
46
47 outperformed the VBM HPS model (ADNI1: 92.3% PPV, 96.1% specificity, 54.6%
48
49 308 sensitivity; ADNI2: 65.2% PPV, 91.5% specificity, 33.3% sensitivity), see Figure 2a. When
50
51 adjusted to the same baseline rate of AD subjects as ADNI1, the PPVs in ADNI2 were
52
53 310 99.2%, 99.3%, and 76.7% for the VCOG, COG, and VBM HPS models respectively.
54

55
56 312 The HPS models consistently outperformed the base SVM classifiers with respect to
57
58 specificity ($p < 0.001$) in the classifications of AD vs CN and pMCI vs sMCI in both ADNI1
59
60 314 PPV ($p < 0.05$) adjusted for a typical prevalence of 33.6% pMCI in a given sample of MCI
61
62
63
64
65

1 subjects [26]. However, these increases in specificity and PPV for the HPS model came at a
2 316 significant cost of reduced sensitivity compared to the base classifier, across all models in
3
4 both ADNI1 and ADNI2 ($p < 0.05$) (Figure 2). Note that this shift towards lower sensitivity
5
6 318 and higher specificity and PPV could be achieved by adjusting the threshold of the SVM
7
8 analysis (see ROC analysis, Figure S1 in supplementary material), and is not unique to the
9
10 320 two-stage procedure we implemented.

11 12 13 **High confidence prediction of progression to AD dementia**

14
15 322 When using the full VCOG features, 87 MCI patients were selected as HPS+ in
16
17 ADNI1, out of which 81 (93.1% PPV) were pMCI within 36 months of follow-up. This
18
19 324 represented a large, significant increase over the baseline rate of progressors in the entire
20
21 ADNI1 MCI sample (37.4%) ($p < 0.001$). This was also a significant increase over the SVM's
22
23 326 predictions, where 83.9% of subjects that it had labeled as hits were true progressors
24
25 ($p < 0.001$). When adjusted to a 33.6% baseline rate of progressors, more typical of MCI
26
27 328 populations, the PPV of HPS+ for prognosis of dementia was 80.4% (93.2% specificity,
28
29 55.1% sensitivity).

30
31 330 We replicated these analyses in the MCI sample from ADNI2 ($N = 235$). Using VCOG
32
33 features, 32 subjects were identified as HPS+, 26 of which progressed to AD dementia within
34
35 332 36 months follow-up (81.2% PPV, specificity of 96.7%, sensitivity of 47.3%, 87.8% PPV
36
37 adjusted to a 33.6% baseline rate). This represented a significantly higher prevalence than the
38
39 334 30.6% baseline rate in the entire ADNI2 MCI cohort ($p < 0.001$). This was also a significant
40
41 increase over the SVM's predictions, where 67.8% of subjects it had labeled as hits were true
42
43 336 progressors ($p < 0.001$). As expected, the HPS+ model had lower sensitivity and higher
44
45 specificity/PPV than the baseline model, both in ADNI1 and ADNI2, and for all three feature
46
47 338 sets (VBM, COG and VCOG), see Figure 2b. The VCOG features also lead to higher PPV
48
49 than VBM and COG features taken independently, both in ADNI1 and ADNI2. That increase
50
51 340 was large and significant between VCOG and VBM (up to 17%) and marginal and
52
53 non-significant between VCOG and COG (up to 8%), see Figure 2b.

54 55 56 342 **Characteristics of MCI subjects with a highly predictive VCOG signature of AD**

HPS+ MCI subjects with the VCOG signature were more likely to be progressors (Figure 3a) compared to non-HPS+ subjects and negative subjects (ADNI1: $p < 0.001$; ADNI2: $p < 0.001$). HPS+ MCI subjects were also more likely to be APOE4 carriers (Figure 3b) (ADNI1: $p < 0.005$; ADNI2: $p < 0.05$). There was no difference in sex across the HPS groupings in the MCI subjects of either the ADNI1 or ADNI2 cohorts (Figure 3c). This was consistent with the whole sample, where there were equal proportions of progressors across both sexes in each dataset (ADNI1: $\chi^2 = 0.015$, $p = 0.90$; ADNI2: $\chi^2 = 0.0002$, $p = 0.99$). The HPS+ class was also significantly enriched for A β -positive subjects in ADNI1 ($p < 0.05$). However, this result was not replicated in the ADNI2 MCI subjects (Figure 3d). Similarly with tau, we found a significant increase in tau-positive subjects in the HPS+ group of ADNI1 ($p < 0.05$), but not in ADNI2 (Figure 3e). We found a significant age difference across the HPS classes in ADNI2 ($F = 5.68$, $p < 0.005$), where the HPS+ subjects were older than the Negative subjects by a mean of 4.4 years. However, age did not differ across the HPS classes in ADNI1 (Figure 3f). Finally, HPS+ subjects had significantly steeper cognitive declines compared to the Non-HPS+ and Negative groups (Figure 3g): there were significant interactions between the HPS groupings and time in ADNI1: (HPS+ $\beta = -0.147$, $t = -7.56$, $p < 0.001$; Non-HPS+ $\beta = -0.055$, $t = -2.46$, $p < 0.05$) and ADNI2 (HPS+ $\beta = -0.194$, $t = -8.69$, $p < 0.001$; Non-HPS+ $\beta = -0.072$, $t = -3.31$, $p = 0.001$). The HPS+ in ADNI1 and ADNI2 respectively gained 1.8 and 2.3 more points each year on the ADAS13 compared to the Non-HPS+ and Negative groups. Note that higher scores on the Alzheimer's Disease Assessment Scale - Cognitive subscale (13 items) (ADAS13) represent worse cognitive function.

COG, VBM and VCOG signatures

The COG signature was mainly driven by scores from the ADAS13, which measures overall cognition, ADNI-MEM, a composite score that measures memory [16], and ADNI-EF, a composite score that measures executive function [27] (coefficients were 5.49, -4.80 and -2.50 respectively). In this model, sex, age, mean GMV, and TIV contributed very little, relative to the cognitive features (Figure 4b). Note that these coefficients should be interpreted as pseudo z-scores as the features had been normalized to zero mean and unit variance.

1
2 374 Almost all grey matter subtypes contributed to the VBM signature. Mean GMV,
3
4 and 3.98 respectively) (Figure 4c). Subtype 1 was characterized by reduced relative GMV in
5
6 376 the occipital, parietal and posterior temporal lobes. Subtype 6 was characterized by reduced
7
8 relative GMV in the temporal lobes, notably the medial temporal regions. We had anticipated
9
10 378 the larger contribution of these two subtypes as they have been described in previous AD
11
12 subtyping work [5,28–30]. Diagnosis (CN, sMCI, pMCI, AD) accounted for a substantial
13
14 380 amount of variance in these subtype weights (subtype 1: $F=8.51$, $p<0.001$; subtype 2:
15
16 $F=34.27$, $p<0.001$). Post-hoc t-tests showed AD subjects had significantly higher weights
17
18 382 compared to CN (Figure 1), making these subtypes associated with a diagnosis of AD
19
20 (subtype 1: $t=2.88$, $p<0.05$; subtype 6: $t=7.68$, $p<0.001$).

21 384 The ADAS13, memory (ADNI-MEM) and executive function (ADNI-EF) scores
22
23 contributed the most to the VCOG HPS signature (coefficients were 6.27, -7.43 and -3.95
24
25 386 respectively, Figure 4a). Of the VBM features, subtypes 2, 3 and 7 contributed the most to the
26
27 signature (coefficients were 1.36, -2.12 and -2.83 respectively). Subtypes 1 and 6, which had
28
29 388 the highest positive weights in the VBM model, were given marginal weights in the VCOG
30
31 model, which is potentially indicative of redundancy with COG features. Subtype 2, which
32
33 390 was associated with AD, was characterized by greater relative GMV in medial parts of the
34
35 parietal and occipital lobes and the cingulate cortex, but less GMV everywhere else. Subtype
36
37 392 3 was characterized by greater relative GMV in the temporal lobes, insula and striatum.
38
39 Subtype 7, which was associated with healthy controls, was characterized by greater relative
40
41 394 GMV in the parietal, occipital and temporal lobes. Note that the weights for subtypes 3 and 7
42
43 were negative in the model, which means that predicted AD and pMCI cases had brain
44
45 396 atrophy patterns that were spatially dissimilar to those subtypes.

47 48 Discussion

49
50 398 We developed a highly precise and specific MRI and cognitive-based model to predict
51
52 AD dementia. Our two-stage predictive model reached 93.2% specificity and 93.1% PPV
53
54 400 (80.4% when adjusted for 33.6% prevalence of progressors) in ADNI1 when classifying
55
56 progressor vs stable MCI patients (within 3 years follow-up). We replicated these results in
57
58 402 ADNI2 where the model reached 96.7% specificity and 81.2% PPV (87.8% adjusted PPV).

1
2 404 With respect to specificity and PPV, these results are a substantial improvement over previous
3 works combining structural MRI and cognition on the same prediction task, that have
4 reported up to 76% specificity and 65% PPV (adjusted for 33.6% prevalence of progressors)
5 [7]. We also report the highest PPV compared to the current state-of-the-art predictive model
6 406 using $A\beta$ PET scans, which reported 74% (adjusted) PPV [8]. Finally, our results also
7 reproduced our past work which developed a model that optimizes specificity and PPV [9].
8
9 408 Our performance is close to the 90% PPV reported by [9], which used a combination of
10 structural and functional MRI measures and a two-stage predictive model, with the limitation
11 of a smaller sample size (N=56 MCI patients) due to limited availability of functional MRI
12 data in ADNI.
13 410
14
15
16
17 412

18
19 An ideal model to predict conversion to AD dementia would have both high
20 sensitivity and specificity. However, the pathophysiological heterogeneity of clinical
21 414 diagnosis will prevent highly accurate prediction linking brain features to clinical trajectories.
22 We argue that, faced with heterogeneity, it is necessary to sacrifice sensitivity to focus on a
23 subgroup of individuals with similar brain abnormalities. The high specificity of our
24 416 two-stage model indeed came at a cost of reduced sensitivity (55.1% in ADNI1 and 47.3% in
25 ADNI2 for classifying pMCI vs sMCI), which is much lower than sensitivity values of
26 64%-95% reported by other groups [9]. The two-stage procedure, based on prediction
27 stability, did not offer gains compared to a simpler SVM model, if the threshold of the SVM
28 418 model could be selected *a priori* to match the specificity of the two-stage procedure (see
29 ROC curves in Figure S1 in supplementary material). The two-stage prediction model offered
30 the advantage of a principled approach to train the prediction model in a high-specificity
31 regime, based on stability. The choice of a L1 regularized logistic regression also lead to a
32 420 compact and interpretable subset of features for the HPS.
33
34
35
36 422
37
38
39
40 424
41
42
43
44 426

45 Favoring specificity over sensitivity is useful in settings where false positives need to
46 be minimized and PPV needs to be high, such as expensive clinical trials. Here, with our HPS
47 428 VCOG model, we report the highest PPVs for progression to AD from the MCI stage (up to
48 87.8%, adjusted for 33.6% prevalence of progressors). Importantly, the proposed HPS+
49 model used tools that are already widely used by clinicians. The present work could be used
50 as a screening tool for recruitment in clinical trials that target MCI subjects who are likely to
51 430 progress to dementia within three years. The implementation of an automated selection
52 algorithm could also result in groups of MCI subjects with more homogeneous brain
53
54
55 432
56
57
58
59 434
60
61
62
63
64
65

1
2 436 pathology. However, we note that HPS+ subjects did not all present with significant amyloid
3
4
5
6 438 burden (92.0% and 68.4% of HPS+ subjects in ADNI1 and ADNI2 respectively, Figure 3),
7
8
9
10
11
12
13
14
15
16
17 444 which means that not all HPS+ individuals are likely to have prodromal AD, even when
18
19
20
21 446 progressing to dementia.

22
23
24
25 448 When we trained our model with cognitive features only, tests for general cognition,
26
27
28
29 450 memory, and executive function were chosen as the strongest predictors of AD dementia. Our
30
31
32
33 452 COG HPS model thus supports previous research that reported general cognition, memory,
34
35
36 454 and executive function as important neuropsychological predictors of dementia [7,18,31,32].
37
38
39
40 456 Compared to the state-of-the-art multi-domain cognition-based predictive model, which
41
42
43
44 458 reported 87.1% specificity and 81.8% PPV (77.5% when adjusted to 33.6% pMCI
45
46
47
48 460 prevalence) [33], our COG HPS model achieved similar performance reaching between
49
50
51
52 462 87.5%-95% specificity and 72.3%-85.1% (adjusted) PPV. As general cognition was the
53
54
55
56 464 strongest feature in our model to predict progression, this supports previous findings that
57
58
59
60 466 MCI patients with deficits across multiple domains are at the highest risk for dementia
61
62
63
64
65 [32,34].

66
67
68
69
70
71
72
73
74
75
76
77
78
79
80
81
82
83
84
85
86
87
88
89
90
91
92
93
94
95
96
97
98
99
100
101
102
103
104
105
106
107
108
109
110
111
112
113
114
115
116
117
118
119
120
121
122
123
124
125
126
127
128
129
130
131
132
133
134
135
136
137
138
139
140
141
142
143
144
145
146
147
148
149
150
151
152
153
154
155
156
157
158
159
160
161
162
163
164
165
166
167
168
169
170
171
172
173
174
175
176
177
178
179
180
181
182
183
184
185
186
187
188
189
190
191
192
193
194
195
196
197
198
199
200
201
202
203
204
205
206
207
208
209
210
211
212
213
214
215
216
217
218
219
220
221
222
223
224
225
226
227
228
229
230
231
232
233
234
235
236
237
238
239
240
241
242
243
244
245
246
247
248
249
250
251
252
253
254
255
256
257
258
259
260
261
262
263
264
265
266
267
268
269
270
271
272
273
274
275
276
277
278
279
280
281
282
283
284
285
286
287
288
289
290
291
292
293
294
295
296
297
298
299
300
301
302
303
304
305
306
307
308
309
310
311
312
313
314
315
316
317
318
319
320
321
322
323
324
325
326
327
328
329
330
331
332
333
334
335
336
337
338
339
340
341
342
343
344
345
346
347
348
349
350
351
352
353
354
355
356
357
358
359
360
361
362
363
364
365
366
367
368
369
370
371
372
373
374
375
376
377
378
379
380
381
382
383
384
385
386
387
388
389
390
391
392
393
394
395
396
397
398
399
400
401
402
403
404
405
406
407
408
409
410
411
412
413
414
415
416
417
418
419
420
421
422
423
424
425
426
427
428
429
430
431
432
433
434
435
436
437
438
439
440
441
442
443
444
445
446
447
448
449
450
451
452
453
454
455
456
457
458
459
460
461
462
463
464
465
466
467
468
469
470
471
472
473
474
475
476
477
478
479
480
481
482
483
484
485
486
487
488
489
490
491
492
493
494
495
496
497
498
499
500
501
502
503
504
505
506
507
508
509
510
511
512
513
514
515
516
517
518
519
520
521
522
523
524
525
526
527
528
529
530
531
532
533
534
535
536
537
538
539
540
541
542
543
544
545
546
547
548
549
550
551
552
553
554
555
556
557
558
559
560
561
562
563
564
565
566
567
568
569
570
571
572
573
574
575
576
577
578
579
580
581
582
583
584
585
586
587
588
589
590
591
592
593
594
595
596
597
598
599
600
601
602
603
604
605
606
607
608
609
610
611
612
613
614
615
616
617
618
619
620
621
622
623
624
625
626
627
628
629
630
631
632
633
634
635
636
637
638
639
640
641
642
643
644
645
646
647
648
649
650
651
652
653
654
655
656
657
658
659
660
661
662
663
664
665
666
667
668
669
670
671
672
673
674
675
676
677
678
679
680
681
682
683
684
685
686
687
688
689
690
691
692
693
694
695
696
697
698
699
700
701
702
703
704
705
706
707
708
709
710
711
712
713
714
715
716
717
718
719
720
721
722
723
724
725
726
727
728
729
730
731
732
733
734
735
736
737
738
739
740
741
742
743
744
745
746
747
748
749
750
751
752
753
754
755
756
757
758
759
760
761
762
763
764
765
766
767
768
769
770
771
772
773
774
775
776
777
778
779
780
781
782
783
784
785
786
787
788
789
790
791
792
793
794
795
796
797
798
799
800
801
802
803
804
805
806
807
808
809
810
811
812
813
814
815
816
817
818
819
820
821
822
823
824
825
826
827
828
829
830
831
832
833
834
835
836
837
838
839
840
841
842
843
844
845
846
847
848
849
850
851
852
853
854
855
856
857
858
859
860
861
862
863
864
865
866
867
868
869
870
871
872
873
874
875
876
877
878
879
880
881
882
883
884
885
886
887
888
889
890
891
892
893
894
895
896
897
898
899
900
901
902
903
904
905
906
907
908
909
910
911
912
913
914
915
916
917
918
919
920
921
922
923
924
925
926
927
928
929
930
931
932
933
934
935
936
937
938
939
940
941
942
943
944
945
946
947
948
949
950
951
952
953
954
955
956
957
958
959
960
961
962
963
964
965
966
967
968
969
970
971
972
973
974
975
976
977
978
979
980
981
982
983
984
985
986
987
988
989
990
991
992
993
994
995
996
997
998
999
1000

For our VBM model, we extracted a number of gray matter atrophy subtypes that recapitulated previously reported subtypes, namely the medial temporal lobe and parietal dominant subtypes [5,28–30], which were associated strongly with a diagnosis of AD dementia. Weights for the parietal dominant and medial temporal lobe subtypes (Subtypes 1 and 6 from Figure 1b, respectively) contributed substantially to the highly predictive signature in the VBM model. The atrophy pattern of subtype 6 is spatially similar to the spread of neurofibrillary tangles in Braak stages III and IV [35], which may support previous findings that tau aggregation mediates neurodegeneration [36]. The contributions of the parietal dominant and medial temporal lobe subtypes in the VBM model are also in line with previous works, which have reported that cortical thickness and volumes of the medial temporal lobes, inferior parietal cortex, and precuneus are strong predictors of progression to dementia [7,37].

1
2 468 markers were stronger features, the VCOG model assigned large negative weights for the
3 structural subtypes 3, which showed greater relative GMV in the temporal lobes, and 7,
4 which showed greater relative GMV in the parietal, occipital, and temporal lobes. This means
5
6 470 that these features were predictive of stable MCI in the VCOG model, in line with previous
7 work showing that atrophy in these regions is predictive of progression to dementia [7,37].
8
9 472 Furthermore, we demonstrated that combining MRI data with cognitive markers significantly
10 improves upon a model based on MRI features alone. This result is again in line with the
11 literature [7,38], yet was shown for the first time for a model specifically trained for high
12
13 474 PPV. Note that in the current study, the predictive model was trained exclusively on images
14 acquired on 1.5T scanners from ADNI1. Good generalization to ADNI2 with 3T scanners
15
16 476 demonstrates robustness of imaging structural subtypes across scanner makes.

17
18
19
20
21 478 The VCOG highly predictive signature might reflect a late disease stage. We looked at
22 the ratio of early to late MCI subjects in the ADNI2 sample (note that ADNI1 did not have
23 early MCI subjects). Of the MCI subjects identified as HPS+ by the VCOG model, 84.4%
24
25 480 were late MCI subjects, compared to a rate of 34.9% of late MCI subjects in the entire
26 ADNI2 MCI sample (Supplementary Figure S3). This approach may not be optimal for early
27
28 482 detection of future cognitive decline. Training a model to classify MCI progressors and
29 non-progressors to dementia could be done in order to capture future progressors in earlier
30
31 484 preclinical stages (e.g. early MCI). Finally, we focused on structural MRI and
32 neuropsychological batteries as features in our models due to their wide availability and
33
34 486 established status as clinical tools. However, we believe adding other modalities such as PET
35 imaging, CSF markers, functional MRI, genetic factors, or lifestyle factors could result in
36
37 488 higher predictive power, especially at earlier preclinical stages of AD.
38
39
40
41
42
43
44
45

46 490 **Conclusion**

47
48 In summary, we found a subgroup of patients with MCI who share a signature of
49
50 492 cognitive deficits and brain atrophy, that put them at very high risk to progress from MCI to
51 AD dementia within a time span of three years. We validated the signature in two separate
52
53 494 cohorts that contained both stable MCI patients and MCI patients who progressed to
54 dementia. The model was able to predict progression to dementia in MCI patients with up to
55
56 496 93.1% PPV and up to 96.7% specificity. The signature was present in about half of all
57
58
59
60
61
62
63
64
65

1
2 498 progressors, demonstrating that gains in PPV can be made by focusing on a homogeneous,
3 yet relatively common subgroup. Our model could potentially improve subject selection in
4 clinical trials and identify individuals at a higher risk of AD dementia for early intervention in
5 500 clinical settings.
6
7
8
9

10 **Competing interests**

11 502 The authors declare no conflicts of interest.
12
13
14

15 **Acknowledgments**

16
17 504 We would like to thank Sylvia Villeneuve, Alexa Pichet-Binette and Jacob Vogel for
18 providing us with data to help start our preliminary analyses for this project. We would like to
19 thank Hien Nguyen for advising us on parts of the statistical analyses.
20 506
21
22

23 Data collection and sharing for this project was funded by the Alzheimer's Disease
24 508 Neuroimaging Initiative (ADNI) (National Institutes of Health Grant U01 AG024904) and
25 DOD ADNI (Department of Defense award number W81XWH-12-2-0012). ADNI is funded
26 by the National Institute on Aging, the National Institute of Biomedical Imaging and
27 Bioengineering, and through generous contributions from the following: AbbVie,
28 Alzheimer's Association; Alzheimer's Drug Discovery Foundation; Araclon Biotech;
29 510 BioClinica, Inc.; Biogen; Bristol-Myers Squibb Company; CereSpir, Inc.; Cogstate; Eisai
30 Inc.; Elan Pharmaceuticals, Inc.; Eli Lilly and Company; EuroImmun; F. Hoffmann-La Roche
31 Ltd and its affiliated company Genentech, Inc.; Fujirebio; GE Healthcare; IXICO Ltd.;
32 Janssen Alzheimer Immunotherapy Research & Development, LLC.; Johnson & Johnson
33 512 Pharmaceutical Research & Development LLC.; Lumosity; Lundbeck; Merck & Co., Inc.;
34 Meso Scale Diagnostics, LLC.; NeuroRx Research; Neurotrack Technologies; Novartis
35 Pharmaceuticals Corporation; Pfizer Inc.; Piramal Imaging; Servier; Takeda Pharmaceutical
36 Company; and Transition Therapeutics. The Canadian Institutes of Health Research is
37 514 providing funds to support ADNI clinical sites in Canada. Private sector contributions are
38 facilitated by the Foundation for the National Institutes of Health (www.fnih.org). The
39 grantee organization is the Northern California Institute for Research and Education, and the
40 516 study is coordinated by the Alzheimer's Therapeutic Research Institute at the University of
41
42
43
44 518
45
46
47
48
49
50
51
52 522
53
54
55
56 524
57
58
59
60
61
62
63
64
65

1 Southern California. ADNI data are disseminated by the Laboratory for Neuro Imaging at the
2 526 University of Southern California.

3
4 The computational resources used to perform the data analysis were provided by
5
6 528 Compute Canada (www.computecanada.org). This project was funded by NSERC grant
7
8 number RN000028 and the Canadian Consortium on Neurodegeneration in Aging (CCNA,
9
10 530 www.ccna-ccnv.ca), through a grant from the Canadian Institutes of Health Research and
11
12 funding from several partners including SANOFI-ADVENTIS R&D. AT is supported by a
13 532 bursary from the Centre de recherche de l'institut universitaire de gériatrie de Montréal and
14
15 the Courtois foundation. CD is supported by a salary award from the Lemaire foundation and
16
17 534 Courtois foundation. PB is supported by a salary award from Fonds de recherche du Québec
18
19 -- Santé and the Courtois foundation.
20
21
22
23
24

25 536 **References**

- 26
27
28 1. Ward A, Tardiff S, Dye C, Arrighi HM. Rate of conversion from prodromal Alzheimer's
29 538 disease to Alzheimer's dementia: a systematic review of the literature. *Dement Geriatr Cogn*
30
31 *Dis Extra*. 2013;3:320–32.
- 32
33 540 2. Visser P-J, Scheltens P, Verhey FRJ. Do MCI criteria in drug trials accurately identify
34
35 542 subjects with predementia Alzheimer's disease? *J Neurol Neurosurg Psychiatry*.
36
37 2005;76:1348–54.
- 38
39 544 3. Scheltens NME, Galindo-Garre F, Pijnenburg YAL, van der Vlies AE, Smits LL, Koene T,
40
41 et al. The identification of cognitive subtypes in Alzheimer's disease dementia using latent
42
43 546 class analysis. *J Neurol Neurosurg Psychiatry*. 2016;87:235–43.
- 44
45 548 4. Murray ME, Graff-Radford NR, Ross OA, Petersen RC, Duara R, Dickson DW.
46
47 Neuropathologically defined subtypes of Alzheimer's disease with distinct clinical
48
49 550 characteristics: a retrospective study. *Lancet Neurol*. 2011;10:785–96.
- 50
51
52 552 5. Hwang J, Kim CM, Jeon S, Lee JM, Hong YJ, Roh JH, et al. Prediction of Alzheimer's
53
54 554 disease pathophysiology based on cortical thickness patterns. *Alzheimer's & dementia*
55
56 (Amsterdam, Netherlands). 2016;2:58–67.
- 57
58 556 6. Dong A, Toledo JB, Honnorat N, Doshi J, Varol E, Sotiras A, et al. Heterogeneity of
59
60 neuroanatomical patterns in prodromal Alzheimer's disease: links to cognition, progression
61
62 and biomarkers. *Brain*. 2017;140:735–47.
- 63
64 7. Korolev IO, Symonds LL, Bozoki AC, for the Alzheimer's Disease Neuroimaging
65
66 Initiative. Predicting Progression from Mild Cognitive Impairment to Alzheimer's Dementia
67
68 Using Clinical, MRI, and Plasma Biomarkers via Probabilistic Pattern Classification. *PLoS*

558 One. 2016;11:e0138866–25.

1
2 8. Mathotaarachchi S, Pascoal TA, Shin M, Benedet AL, Kang MS, Beaudry T, et al.
3 560 Identifying incipient dementia individuals using machine learning and amyloid imaging.
4 Neurobiol Aging. 2017;59:80–90.
5

6
7 562 9. Dansereau C, Tam A, Badhwar A, Urchs S, Orban P, Rosa-Neto P, et al. A brain signature
8 highly predictive of future progression to Alzheimer’s dementia. arXiv preprint arXiv:1712
9 564 08058. 2017;

10
11 10. Bellec P, Lavoie-Courchesne S, Dickinson P, Lerch JP, Zijdenbos AP, Evans A. The
12 566 pipeline system for Octave and Matlab (PSOM): a lightweight scripting framework and
13 execution engine for scientific workflows. Front Neuroinform. 2012;6:7.
14
15

16 568 11. Fonov V, Evans A, Botteron K, Almli CR, McKinstry RC, Collins DL. Unbiased average
17 age-appropriate atlases for pediatric studies. Neuroimage. 2011;54:313–27.
18
19

20 570 12. Ad-Dab’bagh Y, Einarson D, Lyttelton O, Muehlboeck JS, Mok K, Ivanov O, et al. The
21 CIVET image-processing environment: a fully automated comprehensive pipeline for
22 572 anatomical neuroimaging research. Proceedings of the 12th annual meeting of the
23 organization for human brain mapping. 2006;2266.
24
25

26 574 13. Ashburner J. A fast diffeomorphic image registration algorithm. Neuroimage.
27 2007;38:95–113.
28
29

30 576 14. Orban P, Tam A, Urchs S, Savard M, Madjar C, Badhwar A, et al. Subtypes of functional
31 brain connectivity as early markers of neurodegeneration in Alzheimer’s disease. bioRxiv.
32 578 2017;195164.
33

34 15. Zhang X, Mormino EC, Sun N, Sperling RA, Sabuncu MR, Yeo BTT, et al. Bayesian
35 580 model reveals latent atrophy factors with dissociable cognitive trajectories in Alzheimer’s
36 disease. Proc Natl Acad Sci U S A. 2016;113:E6535–44.
37
38

39 582 16. Crane PK, Carle A, Gibbons LE, Insel P, Mackin RS, Gross A, et al. Development and
40 assessment of a composite score for memory in the Alzheimer’s Disease Neuroimaging
41 Initiative (ADNI). Brain Imaging Behav. 2012;6:502–16.
42 584
43

44 17. Gibbons LE, Carle AC, Mackin RS, Harvey D, Mukherjee S, Insel P, et al. A composite
45 586 score for executive functioning, validated in Alzheimer’s Disease Neuroimaging Initiative
46 (ADNI) participants with baseline mild cognitive impairment. Brain Imaging Behav.
47 588 2012;6:517–27.
48
49

50 18. Belleville S, Fouquet C, Hudon C, Zomahoun HTV, Croteau J, Consortium for the Early
51 590 Identification of Alzheimer’s disease-Quebec. Neuropsychological Measures
52 that Predict Progression from Mild Cognitive Impairment to Alzheimer’s type dementia in
53 Older Adults: a Systematic Review and Meta-Analysis. Neuropsychol Rev. 2017;27:328–53.
54 592
55

56 19. Pedregosa F, Varoquaux G, Gramfort A, Michel V, Thirion B, Grisel O, et al. Scikit-learn:
57 594 Machine Learning in Python. J Mach Learn Res. 2011;2825–30.
58
59

60 20. Fan R-E, Chang K-W, Hsieh C-J, Wang X-R, Lin C-J. LIBLINEAR: A library for large
61
62
63
64
65

596 linear classification. *J Mach Learn Res.* 2008;9:1871–4.

1
2
3 598 21. Phipson B, Smyth GK. Permutation P-values should never be zero: calculating exact
4 P-values when permutations are randomly drawn. *Stat Appl Genet Mol Biol.* 2010;9.

5
6 22. Shaw LM, Vanderstichele H, Knapik-Czajka M, Clark CM, Aisen PS, Petersen RC, et al.
7 600 Cerebrospinal fluid biomarker signature in Alzheimer’s disease neuroimaging initiative
8 subjects. *Ann Neurol.* 2009;65:403–13.

9
10 602 23. Jones E, Oliphant T, Peterson P. SciPy: open source scientific tools for Python,
11 <http://www.scipy.org/>. 2001;

12
13
14 604 24. Seabold S, Perktold J. Statsmodels: Econometric and statistical modeling with python.
15 *Proceedings of the 9th Python in Science Conference.* SciPy society Austin; 2010.

16
17 606 25. Pinheiro J, Bates D, DebRoy S, Sarkar D, R Core Team. nlme: linear and nonlinear mixed
18 effects models. R package version 3.1-117, <https://CRAN.R-project.org/package=nlme>. 2018;

19
20
21 608 26. Mitchell AJ, Shiri-Feshki M. Rate of progression of mild cognitive impairment to
22 dementia - meta-analysis of 41 robust inception cohort studies. *Acta Psychiatr Scand.*
23
24 610 2009;119:252–65.

25
26 27. Gibbons LE, Carle AC, Mackin RS, Harvey D, Mukherjee S, Insel P, et al. A composite
27 612 score for executive functioning, validated in Alzheimer’s Disease Neuroimaging Initiative
28 (ADNI) participants with baseline mild cognitive impairment. *Brain Imaging Behav.*
29
30 614 2012;6:517–27.

31
32 28. Noh Y, Jeon S, Lee JM, Seo SW, Kim GH, Cho H, et al. Anatomical heterogeneity of
33 616 Alzheimer disease Based on cortical thickness on MRIs. *Neurology.* 2014;83:1936–44.

34
35
36 29. Park J-Y, Na HK, Kim S, Kim H, Kim HJ, Seo SW, et al. Robust Identification of
37 618 Alzheimer’s Disease subtypes based on cortical atrophy patterns. *Sci Rep.* 2017;7:43270.

38
39
40 620 30. Varol E, Sotiras A, Davatzikos C, Alzheimer’s Disease Neuroimaging Initiative.
41 HYDRA: Revealing heterogeneity of imaging and genetic patterns through a multiple
42 max-margin discriminative analysis framework. *Neuroimage.* 2017;145:346–64.

43
44 622 31. Dickerson BC, Sperling RA, Hyman BT, Albert MS, Blacker D. Clinical prediction of
45 Alzheimer disease dementia across the spectrum of mild cognitive impairment. *Arch Gen
46 624 Psychiatry.* 2007;64:1443–50.

47
48
49 32. Tabert MH, Manly JJ, Liu X, Pelton GH, Rosenblum S, Jacobs M, et al.
50 626 Neuropsychological prediction of conversion to Alzheimer disease in patients with mild
51 cognitive impairment. *Arch Gen Psychiatry.* 2006;63:916–24.

52
53
54 628 33. Belleville S, Gauthier S, Lepage É, Kergoat M-J, Gilbert B. Predicting decline in mild
55 cognitive impairment: A prospective cognitive study. *Neuropsychology.* 2014;28:643–52.

56
57 630 34. Mitchell J, Arnold R, Dawson K, Nestor PJ, Hodges JR. Outcome in subgroups of mild
58 cognitive impairment (MCI) is highly predictable using a simple algorithm. *J Neurol.*

59
60
61
62
63
64
65

2009;256:1500–9.

35. Braak H, Braak E. Neuropathological staging of Alzheimer-related changes. *Acta Neuropathol.* 1991;82:239–59.

36. Spillantini MG, Goedert M. Tau pathology and neurodegeneration. *Lancet Neurol.* 2013;12:609–22.

37. Eskildsen SF, Coupé P, García-Lorenzo D, Fonov V, Pruessner JC, Collins DL, et al. Prediction of Alzheimer’s disease in subjects with mild cognitive impairment from the ADNI cohort using patterns of cortical thinning. *Neuroimage.* 2013;65:511–21.

38. Moradi E, Pepe A, Gaser C, Huttunen H, Tohka J, Alzheimer’s Disease Neuroimaging Initiative. Machine learning framework for early MRI-based Alzheimer’s conversion prediction in MCI subjects. *Neuroimage.* 2015;104:398–412.

Figure Captions

Figure 1. Subtyping procedure and resulting subtypes. a) A hierarchical clustering procedure identified 7 subtypes, or subgroups, of individuals with similar patterns of grey matter topography within the ADNI1 cohort of CN and AD subjects (top). A measure of spatial similarity, called subtype weight, between a single individual's grey matter volume map and the average of a given subtype was calculated for all individuals and all subtypes (bottom). b) Maps of the 7 subtypes showing the distribution of grey matter across all voxels relative to the average. CN* and AD* denote significant associations between the subtype weights and diagnoses of cognitively normal (CN) or Alzheimer's dementia (AD) respectively.

Figure 2. Specificity, sensitivity, and positive predictive value (PPV) for the base SVM and highly predictive signature (HPS) classifiers in the classifications of a) patients with AD dementia (AD) and cognitively normal individuals (CN) and b) patients with mild cognitive impairment who progress to AD (pMCI) and stable MCI (sMCI) in ADNI1 and ADNI2. VBM represents the model trained with VBM subtypes, COG represents the model trained with baseline cognitive scores, and VCOG represents the model trained with both VBM subtypes and cognition. Significant differences are denoted by * for $p < 0.05$ and ** for $p < 0.001$. Positive predictive value was adjusted (PPV (adj)) for a prevalence of 33.6% pMCI in a sample of MCI subjects for both ADNI1 and ADNI2 MCI cohorts.

Figure 3. Characteristics of MCI subjects with the VCOG signature in ADNI1 and ADNI2. We show the percentage of MCI subjects who a) progressed to dementia, were b) APOE4 carriers, c) female, d) positive for $A\beta$ measured by a cut-off of 192 pg/mL in the CSF [22], and e) positive for tau measured by a cut-off of 93 pg/mL in the CSF [22] in each classification (HPS+, Non-HPS+, and Negative). f) Age and g) cognitive trajectories, measured by the Alzheimer's Disease Assessment Scale - Cognitive subscale with 13 items (ADAS13), across the three classes. Significant differences are denoted by * for family-wise error rate-corrected $p < 0.05$.

Figure 4. Coefficients of the high confidence prediction a) VCOG model, b) COG model, and c) VBM model. ADAS13=Alzheimer's Disease Assessment Scale - Cognitive, MEM=ADNI-MEM score; EXEC=ADNI-EF score, BNT=Boston Naming Test, CLOCK=clock drawing test, VBM 1-7=VBM subtype weights, GMV=mean grey matter volume, TIV=total intracranial volume.

1
2
3
4
5
6
7
8
9
10
11
12
13
14
15
16
17
18
19
20
21
22
23
24
25
26
27
28
29
30
31
32
33
34
35
36
37
38
39
40
41
42
43
44
45
46
47
48
49
50
51
52
53
54
55
56
57
58
59
60
61
62
63
64
65

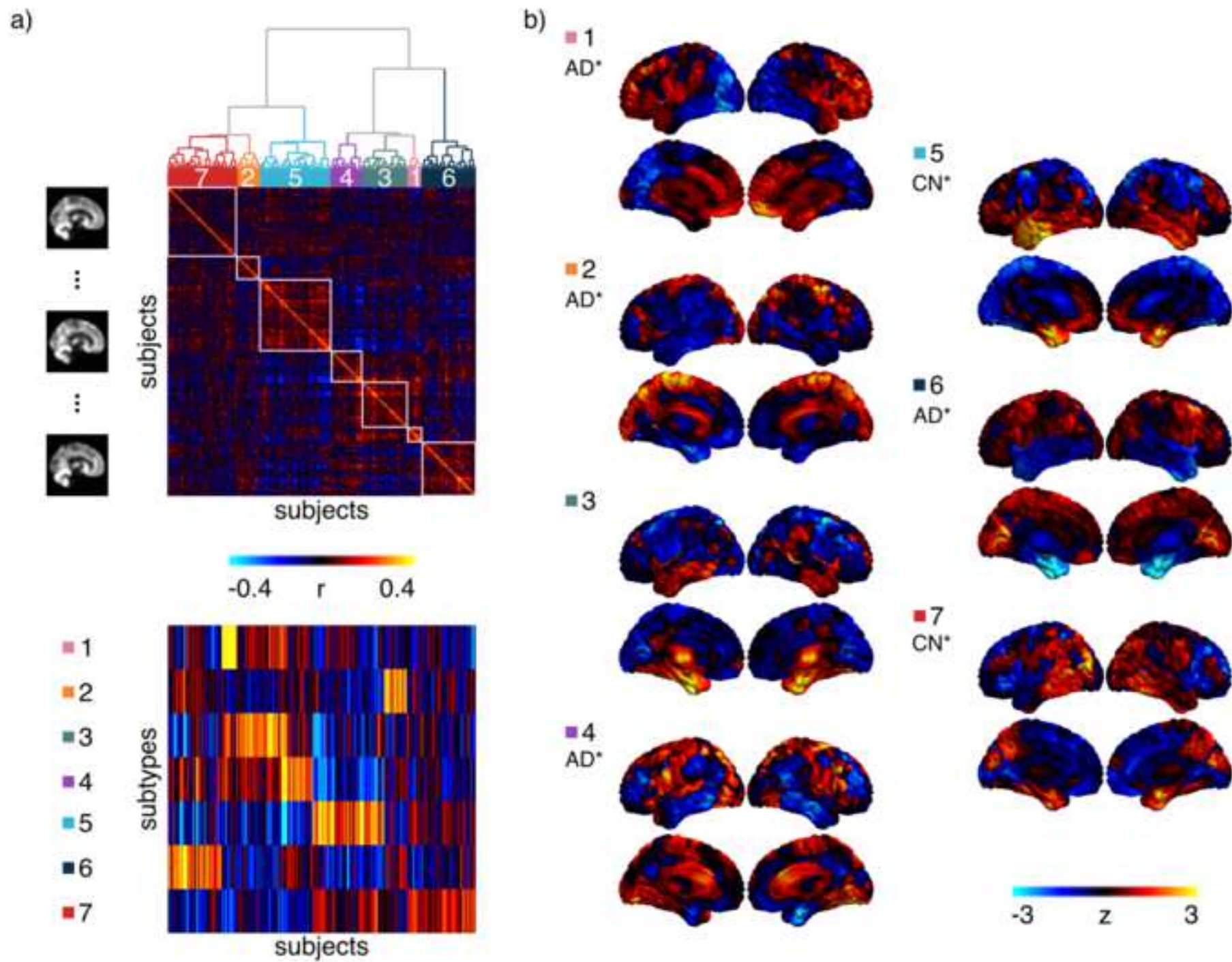
Tables

Table 1. Demographic information for post-QC subjects in ADNI1 and ADNI2.

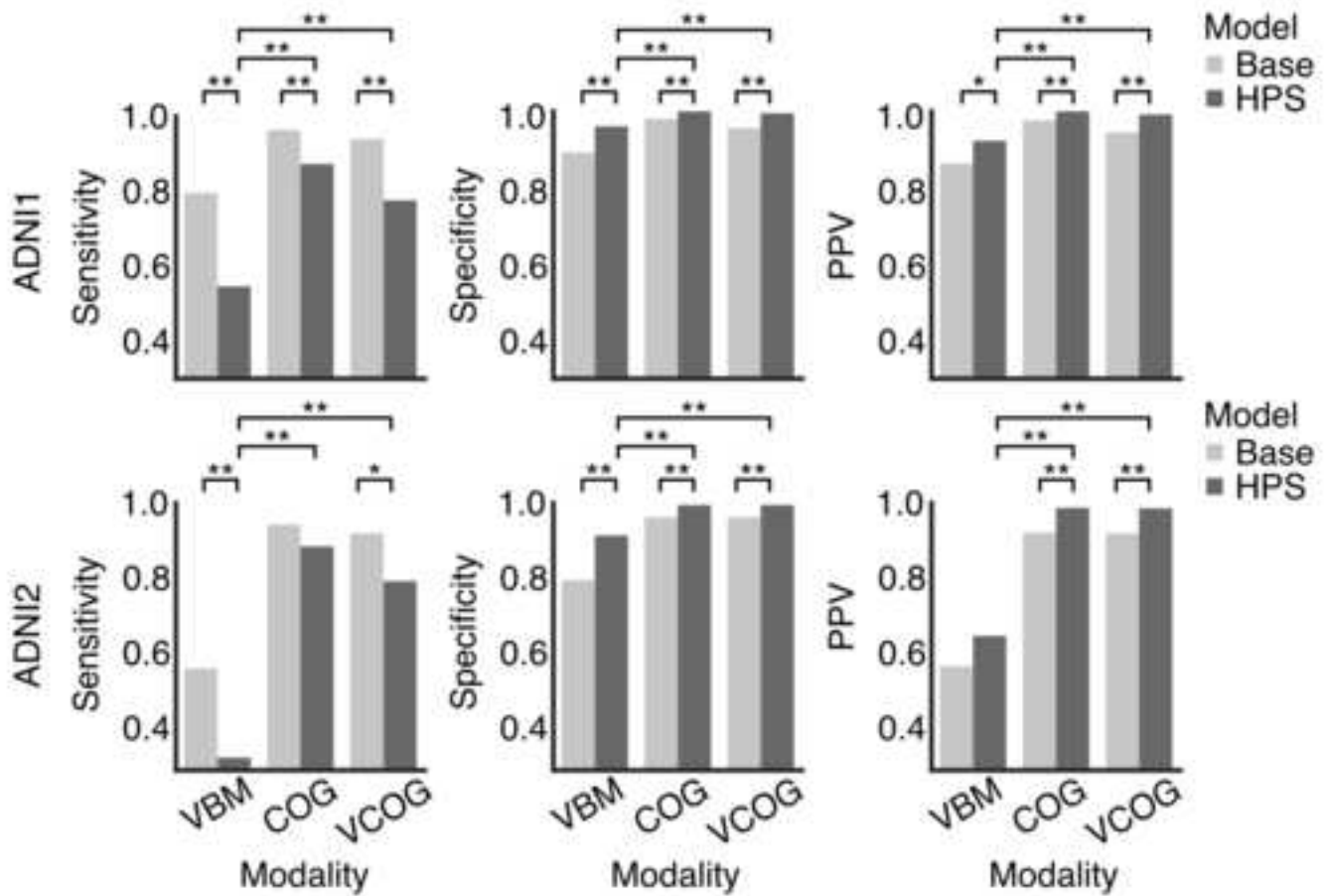
ADNI1	CN	sMCI	pMCI	AD
N	205	88	147	165
Age ± SD	76.1 ± 5.0	74.0 ± 7.6	74.3 ± 7.1	75.4 ± 7.5
Female %	51.7	40.9	40.8	51.5
APOE4+ %	27.8	37.5	68.7	65.4
ADAS13 ± SD	9.5 ± 4.3	14.3 ± 5.5	21.3 ± 5.3	28.6 ± 7.1
MMSE ± SD	29.1 ± 1.0	27.7 ± 1.7	26.7 ± 1.7	23.4 ± 2.0
ADNI2	CN	sMCI	pMCI	AD
N	188	180	55	89
Age ± SD	72.8 ± 6.1	70.8 ± 7.3	72.1 ± 7.1	74.4 ± 7.8
Female %	54.0	47.8	49.1	46.1
APOE4+ %	29.4	35.6	65.4	71.3
ADAS13 ± SD	9.1 ± 4.2	11.8 ± 5.3	21.4 ± 6.5	31.6 ± 8.7
MMSE ± SD	29.1 ± 1.1	28.4 ± 1.6	27.3 ± 1.9	23.1 ± 2.3

ADAS13=Alzheimer's Disease Assessment Scale - Cognitive subscale (13 items);

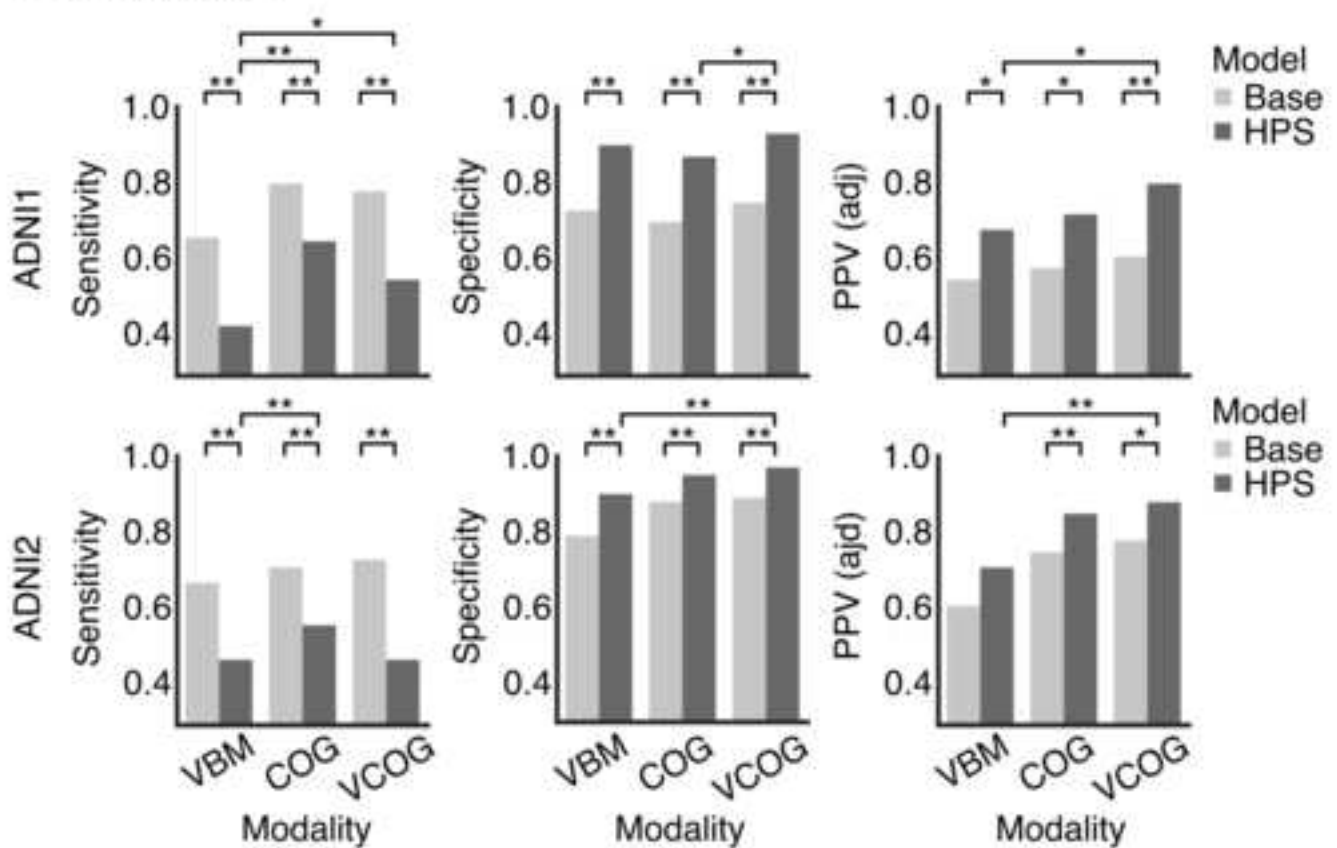
MMSE=Mini Mental State Examination

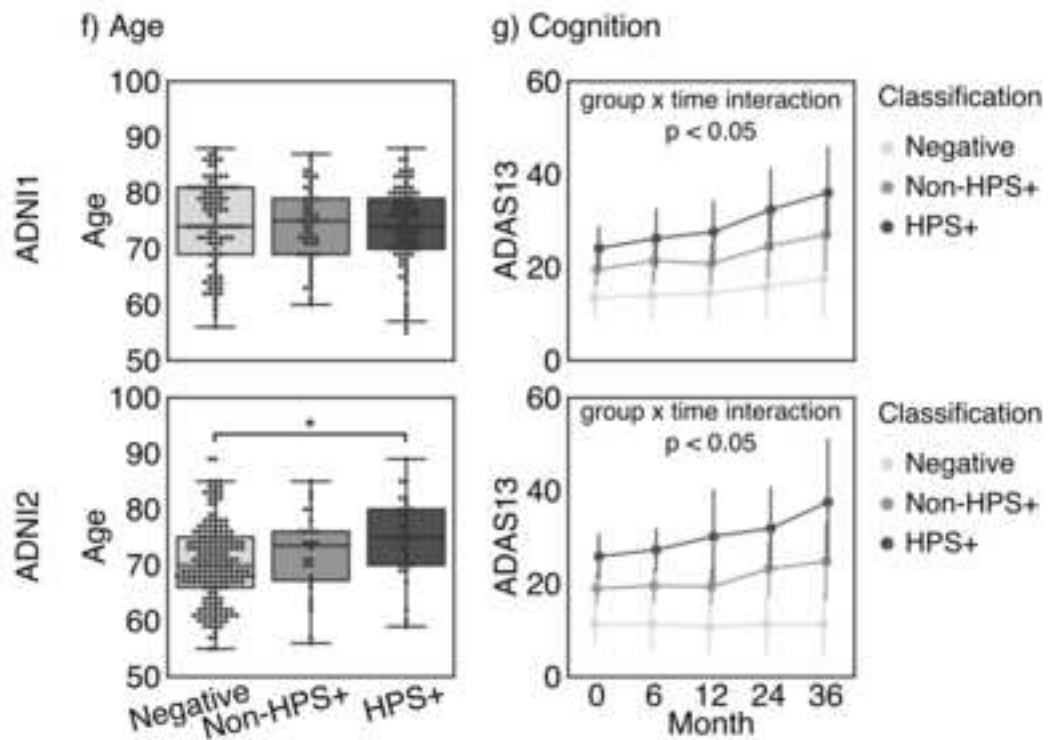
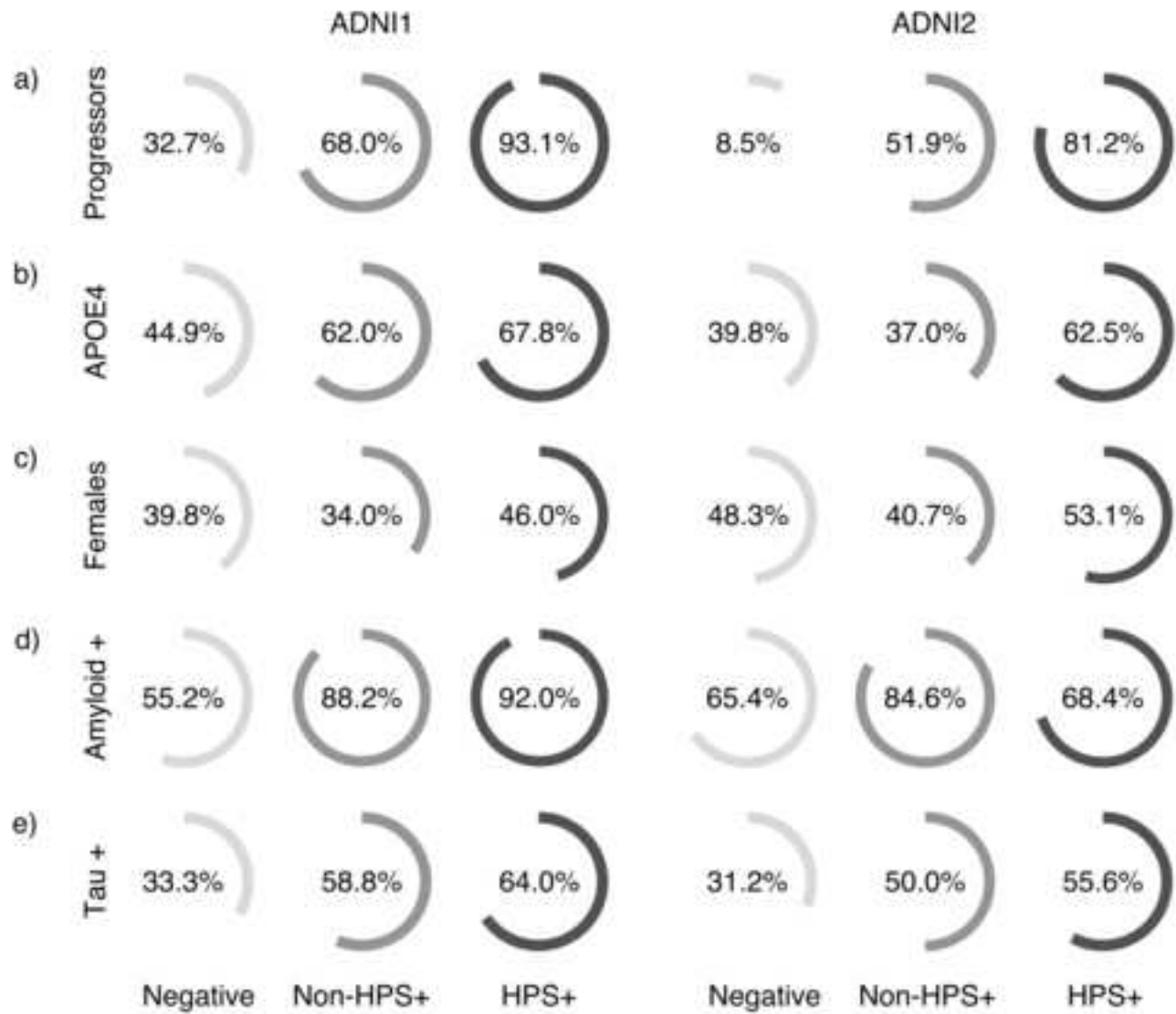


a) AD vs CN

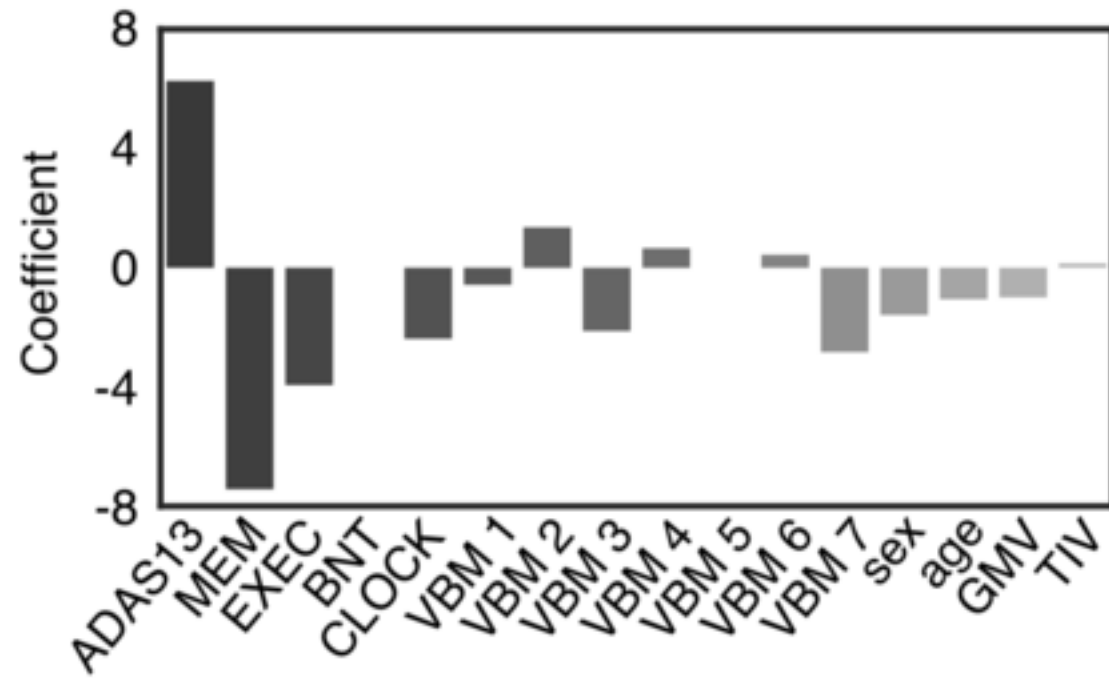


b) pMCI vs sMCI

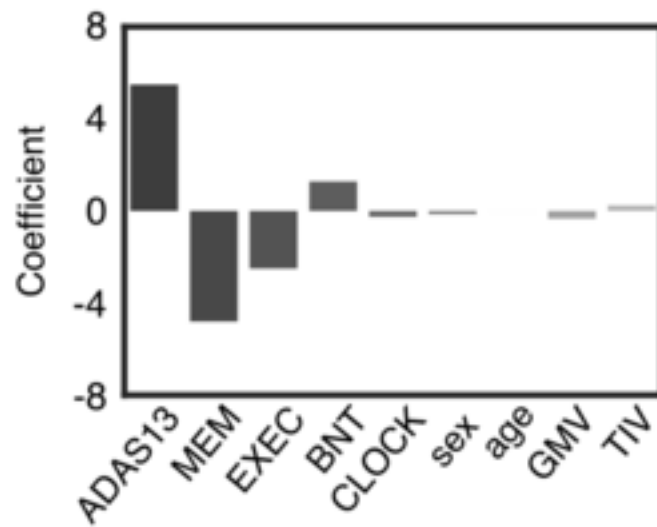




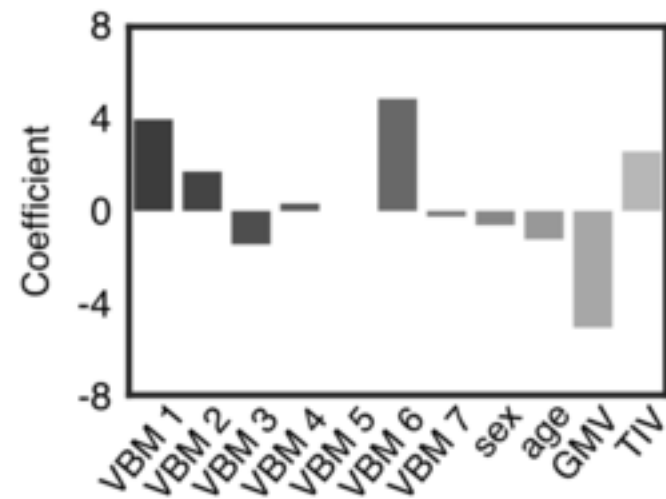
a) VCOG HPS model



b) COG HPS model



c) VBM HPS model





Click here to access/download
Supplementary Material
gigascience_vcog_supplemental.pdf



October 9, 2018

Re: Submission to GigaScience

Dear Editors,

Please find enclosed our revised manuscript titled “A highly predictive signature of cognition and brain atrophy for progression to Alzheimer's dementia” for your consideration.

We have updated our manuscript with the requested information regarding containerization and a simulated dataset.

The simulated dataset is using group-level statistics derived from the ADNI sample, but does not include any participant-level information. As such, it can be freely shared and reused. Importantly, these simulations were designed to replicate the group differences that were identified in the paper using machine learning tools. We have shared a container including all the code and dependencies used in our manuscript, and the reviewers as well as interested readers will be able to reproduce the training and testing of machine learning models from the simulated data. All the code can be executed online via the binder platform, without requiring any local installation or download.

Thank you again for your time and effort in considering our manuscript.

Best regards,

Angela Tam, PhD
On behalf of the co-authors